MEMS-based microsensors using piezoelectric thin films as sensors and actuators

Takeshi Kobayashi[1], Hironao Okada[1], Natsumi Makimoto[1], Syoji Oyama[2], Hiroshi Funakubo[3], Tohishiro Itoh[1], and Ryutaro Maeda[1]

[1] *National Institute of Advanced Industrial Science and Technology (AIST), 1-2-1 Namiki Tsukuba, Ibaraki, 305-8564, Japan*

[2] *Hirose Electric Co., 2-6-3 Nakagawa Chuo, Tuzuki, Yokohama, Kanagawa 224-8540, Japan*

[3] *Tokyo Institute of Technology, 4259 Nagatsuda-cho, Midori-ku, Yokohama, Kanagawa 226-8502, Japan*

Abstract

$Pb(Zr,Ti)O_3$ (PZT) thin films are attractive for the application to MEMS-based microsensors. PZT thin films can act as sensors and actuators through direct and indirect piezoelectric effect. Moreover, it is possible to integrate the piezoelectric thin films for sensor and actuator.

The present study describes MEMS-based electrostatic field sensors using PZT thin films as displacement sensors and vibration actuators. The self-sensitive piezoelectric microcantilevers have $Pb(Zr,Ti)O_3$ (PZT) thin films for sensor and actuator. The MEMS-EFS were fabricated through sol-gel deposition of PZT thin films and MEMS microfabrication process. An output voltage of the PZT thin films for sensor was found to be proportional to the displacement of the microcantilevers. Self-excited vibration of the microcantilevers has been achieved by amplifying and forwarding the output voltage of the PZT thin films for sensor with a band-pass filter circuit. The developed MEMS-EFS can evaluate an electrotatic field of -3 to 3 kV with good linearity.

Keywords: *piezoelectric, PZT, MEMS, electrostatic field sensor*

1. Introduction

$Pb(Zr,Ti)O_3$ (PZT) thin films are attractive for the application to MEMS-based microsensors. PZT thin films can act as sensors and actuators through direct and indirect piezoelectric effect. Moreover, it is possible to integrate the piezoelectric thin films for sensor and actuator. The present study describes MEMS-based elec-

W. Udomkichdecha et al. (eds.), *Materials Challenges and Testing for Manufacturing, Mobility, Biomedical Applications and Climate*,
DOI 10.1007/978-3-319-11340-1_4

trostatic field sensors using PZT thin films as displacement sensors and vibration actuators.

Electrostatic field sensors (EFS) are mainly applied for monitoring the electrostatic field on the exposure drum of copy machines and on the semiconductor wafers and flat panels processed in clean rooms. Miniaturization of EFS through MEMS technology can realize arrayed EFS, which enables 2D-mapping of electrostatic field. MEMS-EFS also realize integration with temperature, humidity and particle sensors, which are capable of multi-sensing wireless sensor nodes for monitoring clean rooms. Although MEMS-EFS based on thermal or electrostatic actuation have been developed [1,2], thermal noise and high voltage derived from such actuation interfere precise measurement of an electrostatic filed. Thus, MEMS-EFS should be based on piezoelectric actuation as well as commercially available ones.

EFS have probes to detect electrostatic field. The relation between the voltage of electrified bodies V_s, the surface of the probes S and the charges induced on the probe Q_s is expressed as

$$Q_s = \varepsilon_{air}\varepsilon_0 \frac{S}{L} V_s, \tag{1}$$

where ε_{air} and ε_0 are permittivity of air and vacuum, L is the distance between the probes and electrified bodies. Since it is difficult to measure Q_s under DC condition, EFS measure V_s by modulating S or L. Commercially available EFS modulate S by the shutter driven by $Pb(Zr,Ti)O_3$ (PZT) ceramics.

In the previous study, we reported MEMS-EFS, which integrate the probes to detect electrostatic field and PZT thin films for actuator into microcantilever [3]. Using the developed MEMS-EFS, we demonstrated the measurement of electrostatic field by modulating L with vibration of the microcantilevers driven at their resonant frequency. Since the resonant frequency can be varied by the intensity of electrostatic filed and environmental conditions such as temperature and humidity, the microcantilevers should be operated by self-excited vibration [4] so that the microcantilevers follow the variation in resonant frequency.

We have already developed self-sensitive piezoelectric microcantilevers, which have PZT thin films for sensor and actuator (sensor PZT and actuator PZT) [5,6]. Then, we have developed MEMS-EFS composed of the probes to detect electrostatic field and the self-sensitive piezoelectric microcantilevers. We have also developed the electronic circuit for self-excited vibration using a band-pass filter. We have successfully demonstrated the measurement of the electrostatic field of -3 to 3 kV with the developed MEMS-EFS operated by self-excited vibration of the self-sensitive piezoelectric microcantilevers.

2. Design and working principle

Figure 1 illustrates the design of the MEMS-EFS developed in the present study. The MEMS-EFS consist of the probes to detect electrostatic field (EFS-probe) and the self-sensitive piezoelectric microcantilevers. The microcantilevers have sensor and actuator PZT. The surfaces of the EFS-probe are located toward electrified bodies as shown in figure 2. When the distance L is varied at the amplitude of l and frequency of f by the actuator PZT, the charges generated on the EFS-probe Q_m are also varied as

$$Q_m = \varepsilon_{air}\varepsilon_0 \frac{S}{L + l\sin 2\pi ft} V_s \,. \tag{2}$$

Assuming $L>>l$, equation (2) can be approximated as

$$Q_m = q\sin 2\pi ft + Q_s \,. \tag{3}$$

This equation means that the charges on the MEMS-EFS are modulated at the amplitude of q. Assuming $q = rQ_s$, eq. (3) is expressed as

$$Q_m = rQ_s \sin 2\pi ft + Q_s \,. \tag{4}$$

Thus, the amplified output voltage of MEMS-EFS V_{EFS} is expressed as

$$V_{EFS} = \frac{ArQ_s \sin 2\pi ft}{C_{total}} + \frac{AQ_s}{C_{total}} \,, \tag{5}$$

where A is an amplifier gain and C_{total} is the total capacitance of all of the components. The amplitude of eq. (5), $V_{EFS,pp}$ is given as

$$V_{EFS,pp} = \frac{ArQ_s}{C_{total}} \,. \tag{6}$$

Using eq. (1), eq. (6) is rewritten as

$$V_{EFS,pp} = Ar\frac{\varepsilon_{air}\varepsilon_0 S/L}{C_{total}} V_s \,. \tag{7}$$

Equation (7) clearly represents that the amplitude of the AC output voltage obtained by amplifying the charge on the EFS-probe is proportional to the voltage of

electrified bodies. Thus, the voltage of electrified bodies can be evaluated by measuring the amplitude of V_{EFS}.

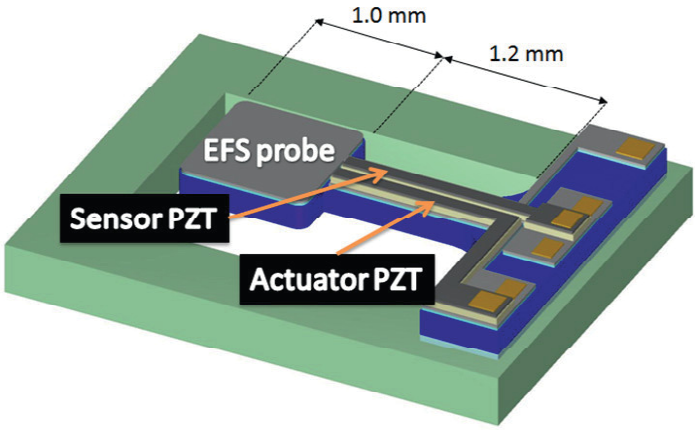

Figure 1. *Design of the MEMS-EFS developed in the present study., which integrate sensor PZT, actuator PZT and probes to detect electrostatic field into microcantilevers. EFS probes are 1 mm-square and cantilever is 1.2 mm-long.*

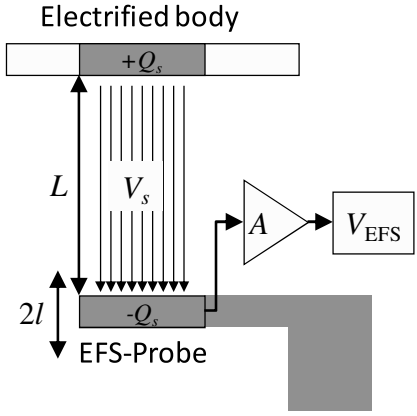

Figure 2. *Schematic of the arrangement of the MEMS-EFS and electrified bodies. The surfaces of the EFS-probe are located toward electrified bodies*

As described above, MEMS-EFS should be operated by self-excited vibration so that the microcantilevers follow the variation in the resonant frequency due to change in the intensity of electrostatic filed and environmental conditions such as temperature and humidity. Figure 3 illustrates the block diagram of the MEMS-

EFS and electronic circuits for self-excited vibration. In self-excited vibration, the output voltage from the sensor PZT, which is amplified and forwarded by the band pass filter, is applied to the actuator PZT. The displacement of the microcantilevers is determined by the source voltage of the band pass filter (5 V at present study). By synchronous detection of the output voltage from the sensor PZT modulated by the band-pass filter and the voltage derived from electric charges induced on the probes, the MEMS-EFS give the output voltage (EFS output) proportional to the intensity of the electrostatic field. The EFS output is calibrated so that the indicator shows the practical voltage of electrified bodies.

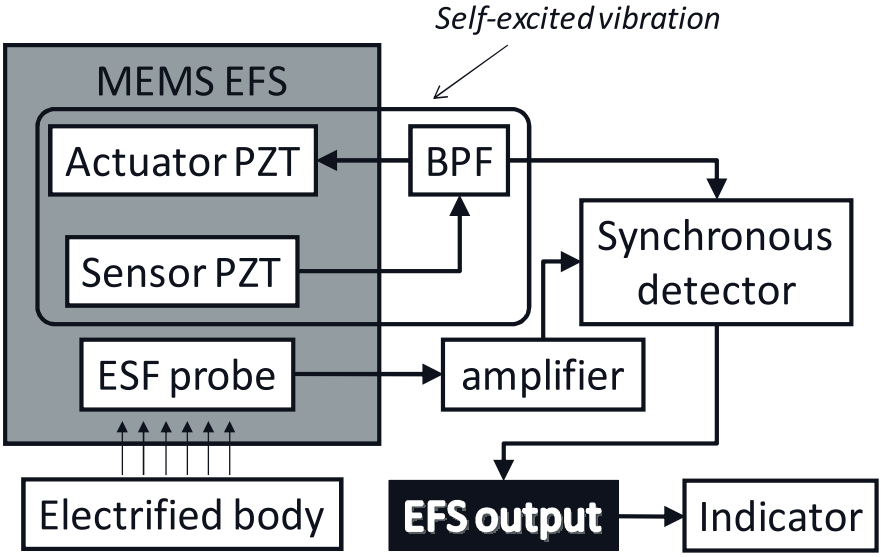

Figure 3. *Block diagram of the MEMS-EFS and electronic circuits for self-excited vibration.*

3. Device fabrication

Figure 4 shows the schematic cross-section of the fabrication process. The designed MEMS-EFS were fabricated from the multilayers of Pt/Ti/PZT/Pt/Ti/SiO_2 deposited on SOI wafers (structural Si: 10 μm, buried SiO_2: 1 μm, substrate Si: 400 μm) through MEMS microfabrication process [7]. The deposition of the multilayers started from thermal oxidation of the SOI wafers followed by Pt/Ti bottom electrodes sputtering. Then, 1.1 μm thick (100)/(001)-oriented $Pb(Zr_{0.52},Ti_{0.48})O_3$ thin films were deposited by sol-gel process [8]. Finally, Pt/Ti top electrodes were sputtered.

After multilayer deposition, Pt/Ti and PZT thin films were etched by Ar-ion etching (Pt/Ti) and wet etching (PZT) through mask 1-3. Next, thermal SiO_2,

structural Si and BOX were etched by RIE with CHF_3 gas (SiO_2) and SF_6 gas (Si) through mask 4. Finally, substrate Si and BOX were etched from backside to release the micro cantilevers and EFS probes. Figure 5(a) shows SEM image of the fabricated MEMS-EFS.

The fabricated MEMS-EFS and amplifiers were mounted on printed circuit boards, which were covered by metal shield caps with an open hole for the probe for electrostatic field detection as shown in figure 5(b). The packaged MEMS-EFS, electronic circuits, and indicators were integrated into plastic cases with dry batteries as shown in figure 5(c). The indicators display measured electrostatic field.

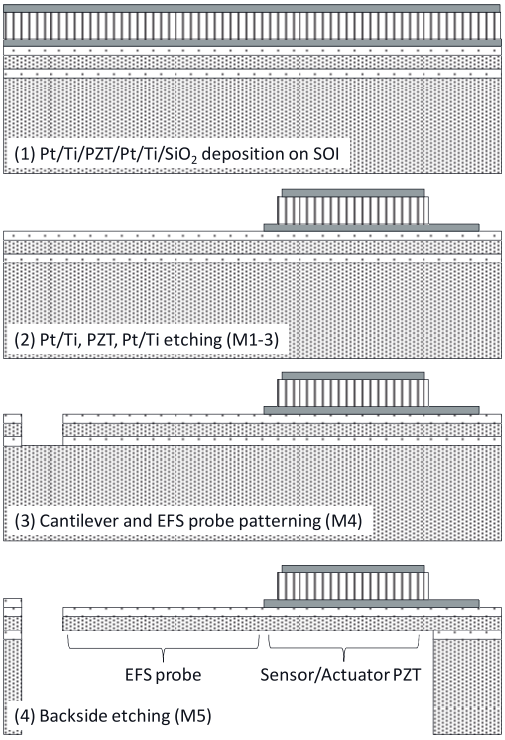

Figure 4. *MEMS microfabrication process for MEMS-EFS. (1)Pt/Ti/PZT/Pt/Ti/SiO_2 deposition on SOI wafer, (2)Pt/Ti, PZT, Pt/Ti etching (Mask 1-3), (3)Cantilever and EFS probe patterning (Mask 4), (4) Backside etching (Mask 5).*

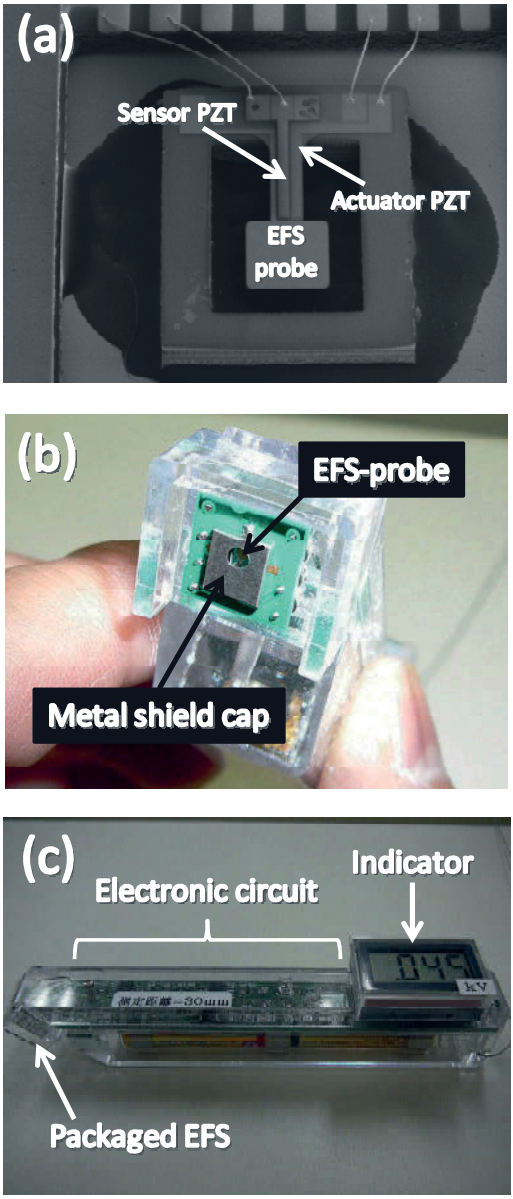

Figure 5. *(a) SEM image of fabricated MEMS-EFS. (b) MEMS-EFS packaged by printed circuit board and metal shield cap. (c)Overview of pencil-type device. EFS is mounted on the top of pencil and electronic circuit is packaged in plastic case. Indicator displays measured electrostatic field.*

4. Test and results

In order to achieve self-excited vibration, the output voltage of the sensor PZT should be proportional to the displacement of the microcantilevers. Thus, we investigated the relation between displacement of the microcantilevers and the output voltage of the sensor PZT by using the similar setup reported in our previous study [5].

AC voltages of 2-10 V_{pp} with 2.5 V of DC bias were applied to the actuator PZT by using a function generator (Tektronix AFG3022, USA). The tip displacement of the vibrating microcantilevers was measured by a laser displacement meter (Graphtec AT1100, Japan). The output voltage of the sensor PZT was directly measured by a digital oscilloscope (Tektronix TDS2004B, USA) by using the AC voltages applied to the actuator PZT as a trigger. The waveforms of the microcantilever displacement and the output voltage of the sensor PZT were simultaneously recorded by the digital oscilloscope.

As shown in figures 6(a) and (b), the output voltage of the sensor was found to be proportional to the microcantilever displacement under both non-resonant (1450 Hz) and resonant conditions (1875 Hz). We have also characterized the relation between the output voltage of the actuator PZT and sensor PZT. Figure 7 shows the output voltage of the sensor PZT, in case the actuator PZT is vibrated under resonant condition (1875 Hz) at 5 V_{pp} by the function generator. The output voltage of the sensor PZT is 0.12 V_{pp} and delays 90 degree compared to the actuation voltage. Figure 8 shows the output voltage of the sensor PZT and that modulated by the band pass filter. The result shows that the output voltage from the sensor PZT is forwarded 90 deg. and amplified to 10 V_{pp}, which indicates the achievement of self-excited vibration.

We have measured an electrified body by using the pencil-type device shown in figure 5 (c). The amplifier shown in figure 3 is tuned so that the indicator shows accurate voltage of the electrified body, where the distance between the MEMEFS and the electrified body should be 30 mm. Figure 9 shows the measurement results. The output of the electrostatic field sensor (EFS output) displayed on the indicator has shown good linearity to the electrostatic field of -3 to 3 kV as we can see in figure 9.

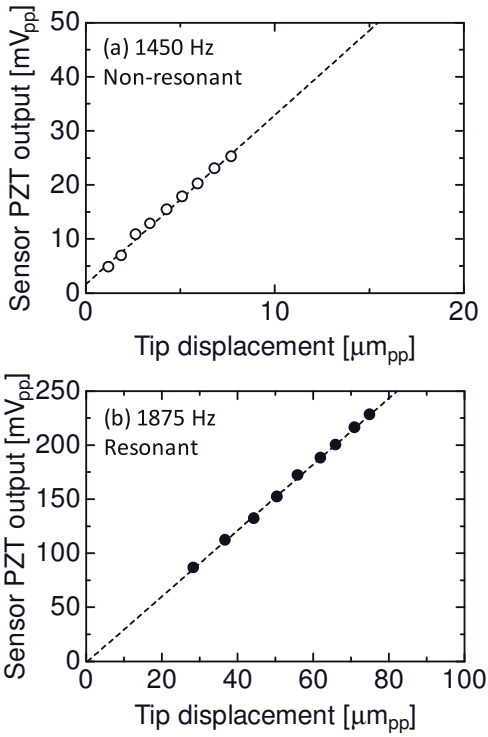

Figure 6. *Relation between the microcantilever displacement and output voltage of the sensor PZT under (a) non-resonant and (b) resonant conditions.*

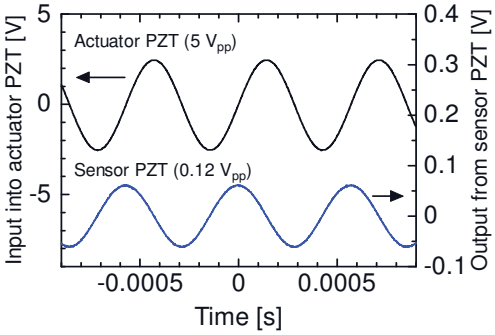

Figure 7. *(top) Input voltage into the actuator PZT from function generator and (bottom) output voltage of the sensor PZT.*

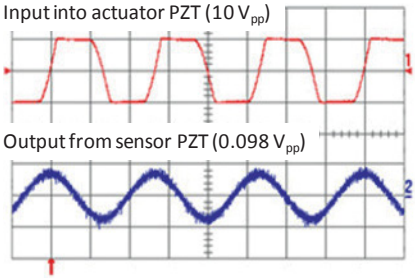

Figure 8. *Input voltage into the actuator PZT obtained by amplifying and forwarding output voltage of the sensor PZT by band pass filter and output voltage of the sensor PZT (0.098 V_{pp}). The result indicates that the microcantilever is under self-excited vibration.*

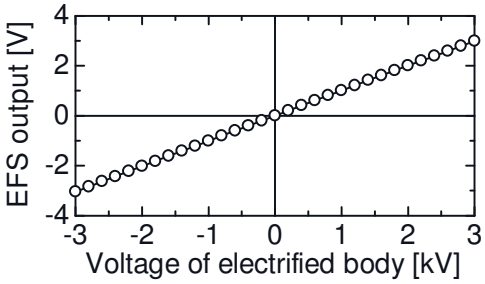

Figure 9. *Output of the electrostatic field sensor (EFS output) as a function of the voltage of electrified body.*

5. Conclusion

We have developed MEMS-based electrostatic field sensors composed of the probes to detect electrostatic field and the microcantilevers with PZT thin films for sensor and actuator. The MEMS-EFS were fabricated through sol-gel deposition of PZT thin films and MEMS microfabrication process. We have also developed electronic circuit using the band pass filter for self-excited vibration of the micro cantilevers. Self-excited vibration of the micro cantilevers has been achieved by amplifying and forwarding the output voltage from the sensor PZT with a band pass filter. By synchronous detection of the output voltage from the sensor PZT modulated by the band-pass filter and the voltage derived from electric charges induced on the probes, the MEMS-EFS give the output voltage proportional to the intensity of the electrostatic field of -3 to 3 kV with good linearity.

Acknowledgement

This research is granted by the Japan Society for the Promotion of Science (JSPS) through the "Funding Program for World-Leading Innovative R&D on Science and Technology (FIRST Program)," initiated by the Council for Science and Technology Policy (CSTP).

References

1. Bahreyni B, Wijeweera G, Shafai C, and Rajapakse A (2008) J Microelectromech Syst 17: 31-36
2. Peng C, Yang P, Zhang H, Guo X, and Xia S (2010) Proc of IEEE sensors 2010 conference: 1183-1186
3. Kobayashi T, Tsaur J, and Maeda R (2008) Jpn J Appl Phys 47: 7533-7536
4. Yabuno H, Kaneko H, Kuroda M, and Kobayashi T (2008) Nonlinear Dynamics 54: 137-149
5. Kobayashi T, Maeda R, and Itoh T (2008) J Micromech Microeng 18: 035025
6. Kobayashi T, Maeda R, and Itoh T (2008) J Micromech Microeng 18: 115007
7. Kobayashi T, Okada H, Masuda T, Maeda R, and Itoh T (2011) Smart Mater Struct 20: 065017
8. Kobayashi T, Ichiki M, Tsaur J, and Maeda R (2005) Thin Solid Films 489: 74-78